



**University of
Zurich**^{UZH}

**Zurich Open Repository and
Archive**

University of Zurich
University Library
Strickhofstrasse 39
CH-8057 Zurich
www.zora.uzh.ch

Year: 2013

Impaired removal of V 8(+) lymphocytes aggravates colitis in mice deficient for B cell lymphoma-2-interacting mediator of cell death (Bim)

Leucht, K ; Caj, M ; Fried, M ; Rogler, G ; Hausmann, M

Abstract: We investigated the role of B cell lymphoma (BCL)-2-interacting mediator of cell death (Bim) for lymphocyte homeostasis in intestinal mucosa. Lymphocytes lacking Bim are refractory to apoptosis. Chronic colitis was induced in Bim-deficient mice (Bim(-/-)) with dextran sulphate sodium (DSS). Weight loss and colonoscopic score were increased significantly in Bim(-/-) mice compared to wild-type mice. As Bim is induced for the killing of autoreactive cells we determined the role of Bim in the regulation of lymphocyte survival at mucosal sites. Upon chronic dextran sulphate sodium (DSS)-induced colitis, Bim(-/-) animals exhibited an increased infiltrate of lymphocytes into the mucosa compared to wild-type mice. The number of autoreactive T cell receptor (TCR) V 8(+) lymphocytes was significantly higher in Bim(-/-) mice compared to wild-type controls. Impaired removal of autoreactive lymphocytes in Bim(-/-) mice upon chronic DSS-induced colitis may therefore contribute to aggravated mucosal inflammation.

DOI: <https://doi.org/10.1111/cei.12137>

Posted at the Zurich Open Repository and Archive, University of Zurich

ZORA URL: <https://doi.org/10.5167/uzh-92838>

Journal Article

Accepted Version

Originally published at:

Leucht, K; Caj, M; Fried, M; Rogler, G; Hausmann, M (2013). Impaired removal of V 8(+) lymphocytes aggravates colitis in mice deficient for B cell lymphoma-2-interacting mediator of cell death (Bim). *Clinical and Experimental Immunology*, 173(3):493-501.

DOI: <https://doi.org/10.1111/cei.12137>

Impaired removal of V β 8⁺ lymphocytes aggravates colitis in mice deficient for BIM

K. Leucht, M. Caj, M. Fried, G. Rogler, M. Hausmann

Division of Gastroenterology and Hepatology, Department of Internal Medicine,
University Hospital of Zürich, 8091 Zürich, Switzerland

Address correspondence to: Martin Hausmann, PhD, Division of Gastroenterology and
Hepatology, Department of Internal Medicine, University Hospital of Zürich, Raemistrasse
100, 8091 Zurich, Switzerland,

Fax: +41 44 255 9496

Phone: +41 44 255 9916

E-mail: martin.hausmann@usz.ch

Disclosure: KL, MK, MF and MH have no conflict of interest to disclose.

GR discloses grant support from Abbot, Ardeypharm, Essex, FALK,
Flamentera, Novartis, Roche, Tillots, UCB and Zeller.

Financial support: This work was supported by the Swiss National Foundation (MH) and
the Broad Medical Research Program (MH).

Running head: Impaired lymphocyte removal in *Bim*^{-/-}

Word count: 3725

List of how each author was involved with the manuscript:

- study concept; Martin Hausmann
- acquisition of data; Katharina Leucht, Michaela Krebs, Martin Hausmann
- critical revision of the manuscript; Michael Fried, Gerhard Rogler

Abstract

Introduction: We investigated the role of BCL-2-interacting mediator of cell death (BIM) for lymphocyte homeostasis in intestinal mucosa. Lymphocytes lacking BIM are refractory to apoptosis.

Materials and methods: Chronic colitis was induced in *Bim* deficient mice (*Bim*^{-/-}) with dextran sulfate sodium (DSS).

Results: Weight loss and colonoscopic score were significantly increased in *Bim*^{-/-} mice as compared to wildtypes (wt). As BIM is induced for killing of autoreactive cells we determined the role of BIM in regulation of lymphocyte survival at mucosal sites. Upon chronic DSS-induced colitis *Bim*^{-/-} animals exhibited an increased infiltrate of lymphocytes into the mucosa compared to wt. The number of autoreactive TCR V β 8⁺ lymphocytes was significantly higher in *Bim*^{-/-} mice compared to wt controls.

Discussion: Impaired removal of autoreactive lymphocytes in *Bim*^{-/-} mice upon chronic DSS-induced colitis may therefore contribute to aggravated mucosal inflammation.

Keywords: BIM; autoreactive TCR; V β 8⁺ lymphocytes; apoptosis

Introduction

Pro-survival B-cell lymphoma (BCL)-2 interacts with pro-apoptotic BCL-2-interacting mediator of cell death (BIM). BIM is sequestered to microtubules [1]. By this BIM can be separated from BCL-2. Upon apoptotic stimuli, like UV irradiation and growth factor withdrawal, BIM translocates to BCL-2 and neutralizes its anti-apoptotic activity. This process does not require caspase activity and therefore constitutes an initiating event in apoptosis signalling. BIM was suggested to have an increased prevalence of phosphorylation sites. BIM is phosphorylated and targeted for degradation by the proteasome [2].

Inactivation of BCL-2 has been suggested to be the key to the ability of BIM to induce apoptosis. However, an alternative model argues that some forms of BIM can also bind directly to the other pro-apoptotic proteins BAX and BAK in order to initiate apoptosis [3]. BAX and BAK act by forming pores in the mitochondrial membrane finally triggering apoptosis. Other BH3-only proteins like BMF, BAD, NOXA and PUMA are considered to act as sensitizer which bind the pro-survival BCL-2 protein and thereby displace BIM from BCL-2 to promote cell death [4].

BIM transduces death signals not only after its release from the actin cytoskeleton, but also by activation of its transcription. *BIM* transcription is induced by transforming growth factor- β (TGF β)-driven apoptosis in a number of cell types [5]. TGF β -induced autophagy potentiates the induction of the pro-apoptotic BIM by the stress-responsive transcription factor CHOP upon growth factor withdrawal [6].

Bcl-2 and Bim play a critical role in the establishment and maintenance of the immune system by regulating the survival of lymphocytes by apoptosis. The effect of the interaction of Bcl-2 and Bim is dependent on the cell type and/or is tissue specific: Bcl-2 promotes the survival of naïve T cells [7]. In turn, naïve T cells from

Bim^{+/-} *Bcl-2*^{-/-} mice die at an accelerated rate *in vitro*. Bcl-2 is critical to prevent pro-apoptotic effects of Bim in naïve CD8⁺ T cells *in vivo* but other molecules than Bcl-2 may antagonize Bim in CD4⁺ cells. Bim controls T cell numbers in the periphery by promoting apoptosis and /or decreasing thymic production. Bim-deficient mice have elevated numbers of normal single positive T cells in the periphery [8]. BIM is a primary trigger for killing autoreactive B cells during their development [9]. In contrast, Bcl-2 is required less for the generation and/or maintenance of memory T cells [7].

Bcl-2 and Bim play a critical role in controlling immune responses by regulating the survival, expansion and contraction of lymphocytes by apoptosis. The majority of activated T cells die at the end of a T cell response. Activated T cells exhibit decreased levels of Bcl-2 at the peak of the T cell response, just before they began to die *in vivo* [10]. A decrease of the pro-survival protein Bcl-2 contributes to apoptosis of activated T cells [11]. Bim deficiency prevents the death of activated T cells *in vitro* and *in vivo*, suggesting that the protective effects of Bcl-2 acts solely to neutralize Bim [11].

Thymocytes can be negatively selected by exposure to anti-CD3 antibody, which aggregates the TCR-CD3 complex and kills the CD4⁺CD8⁺ population *in vivo* and *in vitro*. Thymocytes lacking the pro-apoptotic Bim are refractory to TCR ligation-induced killing [12]. Stimulation with the superantigen *Staphylococcus* enterotoxin B (SEB) activates most T cells that express a variable region (V)-β8 TCR. Addition of SEB to fetal thymic organ cultures deletes most developing TCRVβ8⁺ thymocytes. In contrast, TCRVβ8⁺ escaped apoptosis in SEB-treated thymic lobes from *Bim*^{-/-} embryos [12].

Lymphocytes from *Bim*^{-/-} mice were found to be relatively resistant to apoptosis upon BH3-only mimetics compared to those from wt mice. Presence of BIM

differently affected apoptosis of Treg cells when compared to CD4⁺8⁺ thymocytes. Loss of pro-apoptotic BIM rescued Treg cells from intrinsically initiated apoptosis [13]. Next to the role of BIM for apoptosis of Treg cells absence of BIM also affects phenotype and function of Treg cells in a manner that indicates loss of function.

Exaggerated response of T lymphocytes to luminal antigens is suggested to increase intestinal inflammation in inflammatory bowel disease (IBD). In Crohn's disease (CD), mucosal T cells escape normal apoptosis. The lifespan of antigen-primed T cells is extended and an abnormal population of activated cells is retained within the mucosal compartment.

Enhanced expression of the pro-survival proteins BCL-2 and BCL-x_L were determined in lamina propria T cells of patients with CD compared to controls. Lamina propria T cells in CD show activation of the STAT-3 signalling pathway mediated by IL-6. Activation of STAT-3 is followed by the induction anti-apoptotic genes such as *BCL-2* and *BCL-x_L* [14]. Resistance of CD T cells to multiple apoptotic signals is associated with increased BCL-2 expression. An abnormal BCL-2 expression in lamina propria mononuclear cells from patients with CD was demonstrated [15]. A significantly higher BCL-2/BAX ratio in CD mucosa compared to control was reported [16]. These data are consistent with a recent report showing significant resistance to Fas-induced apoptosis of peripheral T-cells from CD patients [17]. However, no significant difference in the BCL-2/BAX ratio in peripheral blood from CD patients compared to control was reported.

Our own studies on apoptosis of lymphocytes in the gut-mucosa revealed that cell death in Peyer's patches is dependent on the pro-apoptotic protein BIM. Based on these findings we investigated the role of BIM for cell death of lymphocytes in mice under inflammatory conditions.

Material and Methods

Induction and treatment of chronic dextran sulfate sodium (DSS) colitis - B6.129-Bcl2l1^{tm1.1Ast}/J (*Bim*^{-/-}) mice were kindly provided by Professor Dr. Andreas Villunger (Division for Developmental Immunology, Innsbruck Medical University). *Bim*^{-/-} mice were backcrossed for at least 12 generations [18]. Mice weighing 20-25 g were used for the experiments and housed in individually ventilated cages (IVC). All animals were housed for at least three weeks prior to testing in a specific pathogen free (SPF) facility. Chronic colitis was induced as described previously [19]. During a cycle of chronic colitis mice received either 2.5 % DSS in drinking water or drinking water alone over seven days. In between, the animals were given 14 day periods of recovery. Female mice received 3-5 cycles of DSS treatment as described. Mice were killed 2 weeks after completion of the last DSS cycle.

Assessment of colonoscopy and histological score in mice - Animals were anesthetized i.p. with a mixture of 90-120 mg ketamine (Narketan 10 %, Vétoquinol AG, Bern Switzerland) and 8 mg xylazine (Rompun 2 %, Bayer, Switzerland) per kg body weight and examined with the Tele Pack Pal 20043020 (Karl Storz Endoskope, Germany) and scored with a murine endoscopic index of colitis severity (MEICS) as described previously [20].

Assessment of histological score in mice - For the assessment of the histological scores 1 cm of the distal third of the colon was removed and scored as described [19, 21].

RNA extraction and quantitative real time PCR - Total RNA was extracted from murine tissue using the RNeasy Mini Kit and the automated sample preparation system QIAcube as proposed by the manufacturer (Qiagen, Switzerland). mRNA was reverse transcribed into cDNA using High Capacity cDNA Reverse Transcription Kit (Applied Biosystems, USA). *Bim* and *iNos* gene expression was determined with a TaqMan[®] Gene Expression Assay (#Mm00437796_m1 and #Mm01309893_m1 Applied Biosystems). GAPDH gene expression was measured as endogenous control (#4352339E; Applied Biosystems) and used for calculation of relative mRNA expression by the $\Delta\Delta C_t$ method. All samples were analyzed as triplicates.

Western blot - Samples were lysed in M-PER protein extraction buffer (Thermo Fisher Scientific, Perbio Science, Switzerland). Proteins were separated on 10 % polyacrylamide gels with Tris/SDS running buffer and transferred onto nitrocellulose (Invitrogen). Membranes were blocked with 5 % milk, 3 % BSA and 0.1 % Tween 20 and incubated rabbit anti-mouse iNOS (cell signaling, # 2977S). Horseradish peroxidase-conjugated secondary antibody: goat anti-rabbit (#sc-2004; Santa Cruz; diluted 1:3'000). β -actin was used as a loading control.

Immunofluorescence (IF) - Murine colonic tissue samples were fixed in 3.7 % formaldehyde, embedded in paraffin and cut. Demasking for TCR V β 8 IF was performed using DAKO target retrieval solution (# S2367, pH 9) and proteinase K (DAKO, Denmark). 1 % BSA in PBS was used to block unspecific binding sites. Primary antibodies: FITC-labeled mouse anti-mouse TCR V β 8 (# BD 553861). Nuclei were visualized with diamidino phenylindole (DAPI; Invitrogen; final concentration 3 μ M). The sections were mounted with fluorescent mounting medium (DAKO) and analyzed by confocal laser scanning microscopy (SP5, Leica, Switzerland).

Statistical analysis - Real time PCR data were calculated from triplicates. Statistical analyses were performed using PASW statistics 18.0 (SPSS Inc., USA). Kruskal-Wallis non-parametric analysis of variance and Bonferroni-corrected Mann-Whitney rank sum test were applied for animal experiments. Box plots express median, 25 % quartiles around median, minimum and maximum. One-Way ANOVA and Tukey Post Hoc test were used for cell culture experiments. Bars represent mean values with Whiskers displaying standard deviation. Differences were considered significant at $p < 0.05$ (*), highly significant at $p < 0.01$ (**) and very highly significant at $p < 0.001$ (***). Luminescence of Western was quantified densitometrically with OptiQuant (Packard Instrument, USA).

Ethical Considerations

The experimental protocol was approved by the local Animal Care Committee of the University Zurich (146/2009) and has been granted by the Swiss National Science Foundation (SNF 31003A_127247) to M Hausmann and the Broad Medical Research Foundation (IBD-0324) to M Hausmann.

Results

Bim^{-/-} mice develop rectum prolapses. Previous experimental evidence indicated that the loss of *Bmf* causes defects in uterovaginal development, e.g. an imperforate vagina and hydrometrocolpos [22]. We analyzed phenotypic abnormalities of *Bim*^{-/-} animals in the anal. Animals were kept in IVC under SPF conditions. Rectum prolapses were found in 18 of 104 *Bim*^{-/-} animals (figure 1 A - B) which have not been used for breeding. Anal bleeding was observed in those. No increase in collagen deposition in *Bim*^{-/-} colon was detectable by Sirius Red and Elastica von Giesson staining (not shown). Analysis of the length of collagen fibrils by polarized light microscopy also revealed no change in *Bim*^{-/-} animals with prolapse compared to wt mice without prolapse. Colon length was not altered in *Bim*^{-/-} animals compared to wt mice (8.0 ± 1.0 , n = 18 vs. 7.9 ± 0.8 , n = 15 respectively, not shown). Transepithelial resistance measured in 1 - 2 cm distance from the distal end of the colon. Transepithelial resistance was not altered in *Bim*^{-/-} animals compared to wt mice ($35 \pm 5 \Omega \times \text{cm}^2$, n = 5 vs. $39 \pm 6 \Omega \times \text{cm}^2$, n = 5 respectively, female mice without rectum prolapse, not shown).

Previous experimental evidence reported impaired cell death of lymphocytes in the absence of BIM [18]. We analyzed peripheral blood from seven wt controls and seven *Bim*^{-/-} mice on an ADVIA 2120i hematology system (Siemens AG, Germany). Total number of leukocytes was significantly increased in *Bim*^{-/-} mice compared to wt controls ($8.21 \pm 2.52 \times 10^9$ cells/L vs. $1.66 \pm 0.48 \times 10^9$ cells/L, $p < 0.001$). Total numbers of lymphocytes ($6.61 \pm 2.90 \times 10^3$ cells/ μL vs. $1.24 \pm 0.34 \times 10^3$ cells/ μL , $p < 0.001$), neutrophilic leukocytes ($1.20 \pm 1.27 \times 10^3$ cells/ μL vs. $0.28 \pm 0.25 \times 10^3$ cells/ μL , $p < 0.001$) and eosinophilic leukocytes ($0.24 \pm 0.20 \times 10^3$ cells/ μL vs. $0.06 \pm 0.03 \times 10^3$ cells/ μL , $p < 0.001$) were significantly increased in *Bim*^{-/-} mice

compared to wt controls. In contrast the proportion of monocytes was significantly decreased in *Bim*^{-/-} mice compared to wt controls (0.91 ± 0.30 vs. 2.73 ± 1.24 , $p < 0.001$). Consistently, we observed a significant difference in the spleen weight between *Bim*^{-/-} and wt mice (spleen weight / body weight 7.7 ± 0.9 mg/g, $n = 10$ vs. 4.2 ± 0.4 mg/g, $n = 5$; respectively, $p < 0.05$, figure 3 A).

Intestinal inflammation is aggravated in Bim^{-/-} mice upon chronic DSS-colitis. As we found rectum prolapses, anal bleeding and a significant increase in the spleen weight in our *Bim*^{-/-} animals we focused on BIM-dependence of intestinal inflammation and lymphocyte-apoptosis in chronic DSS-induced colitis. Upon chronic DSS-induced colitis, weight loss of *Bim*^{-/-} mice was significantly higher as compared to wt during the last days before the animals were sacrificed (figure 2A). The macroscopic mucosal damage was assessed by colonoscopy and a murine endoscopic index of colitis severity (MEICS) [20]. Mucosa from female *Bim*^{-/-} mice and wt without colitis displayed a smooth and transparent mucosa with a normal vascular pattern (0.4 ± 0.4 , $n = 7$ vs. 0.2 ± 0.4 , $n = 5$ respectively; not shown). After induction of chronic colitis the colon of both *Bim*^{-/-} mice and wt appeared with an intransparent, thickened, more granular mucosa, and an altered vascular pattern. *Bim*^{-/-} animals exhibited significantly higher MEICS score compared to wt mice (5.1 ± 1.7 , $n = 7$ vs. 2.7 ± 1.8 , $n = 5$ respectively; figure 2B).

Spleens of healthy wt mice were significantly smaller than those of *Bim*^{-/-} animals. Upon DSS, the spleen weight significantly increased in wt mice ($p < 0.05$) and highly significantly in *Bim*^{-/-} animals ($p < 0.01$, figure 3 A). Induction of chronic colitis was followed by a typical reduction of colon length. Shortening of the colon was significant in DSS-receiving *Bim*^{-/-} animals compared to the respective controls (8.1 ± 0.5 cm upon water, $n = 5$, vs. 7.0 ± 0.8 cm upon DSS, $n = 5$ for wt animals. 8.8 ± 0.4 cm

upon water, $n = 7$, vs. 7.8 ± 0.5 cm upon DSS, $n = 7$, $p < 0.05$ for *Bim*^{-/-} mice; figure 3 B). Increase of spleen weight upon chronic DSS-induced colitis correlated with a decrease in colon length for both wt controls and *Bim*^{-/-} mice ($p < 0.05$). Combining data from wt controls and *Bim*^{-/-} mice upon both water and DSS no significant relationship between spleen weight and colon length could be determined because of the significant difference in the spleen weight between wt and *Bim*^{-/-} in mice without inflammation.

Also on a microscopic level, for *Bim*^{-/-} mice a more severe colitis was found compared to wt. In female animals without chronic DSS-induced colitis, the knockout of *Bim* did not alter the total histological score compared to wt (1.2 ± 0.6 vs. 1.3 ± 0.6 respectively; figure 3 C). The total histological score for *Bim*^{-/-} mice with an induced chronic colitis was significantly increased compared to the water-treated mice. The score for epithelial damage considering crypt morphology and loss of goblet cells remained unchanged when comparing DSS-receiving *Bim*^{-/-} and wt (figure 3 C, white bars). In contrast, *Bim*^{-/-} animals with chronic colitis exhibited a significantly increased inflammatory infiltrate of lymphocytes into the mucosa and submucosa compared to wt (4.4 ± 0.8 vs. 3.1 ± 1.0 respectively; $p < 0.05$; figure 3 C, light grey bars). This also led to a significantly higher total histological score for *Bim*^{-/-} mice with chronic colitis compared to wt (6.7 ± 1.4 vs. 4.9 ± 0.4 respectively; $p < 0.05$; figure 3 C, dark grey bars).

The results were confirmed in a second experiment of chronic DSS-induced colitis in female mice ($n = 5$ each group, not shown). In a third experiment in male *Bim*^{-/-} mice, similar data were obtained ($n = 5$ each group, not shown). In these animals a more severe inflammation for *Bim*^{-/-} animals compared to wt was determined upon chronic DSS-induced colitis.

Impaired removal of autoreactive lymphocytes in $Bim^{-/-}$ mice upon chronic DSS-induced colitis contributes to aggravated mucosal inflammation. As lymphocyte killing is impaired in $Bim^{-/-}$ mice and loss of function is indicated for Tregs from those animals, we focused on the induction of apoptosis in lymphocytes in chronic DSS-induced colitis in $Bim^{-/-}$ animals compared to wt. The histological score shows a significantly increased lymphocyte infiltration in the intestinal mucosa in $Bim^{-/-}$ animals compared to wt upon chronic DSS-induced colitis.

First, we isolated Peyer's patches by excising whole lymph nodes together with adherent mucosal tissue. We could show increased gene expression levels for *Bim* in wt when animals had developed a chronic colitis (control: 1.1 ± 0.3 , $n = 5$; DSS: 1.5 ± 0.6 , $n = 5$; figure 3 D).

As TCR V β 8⁺ T cells from $Bim^{-/-}$ mice were found resistant to enterotoxin-induced deletion [11] and apoptosis of TCR V β 8⁺ T cells but not TCR V β 6⁺ T cells is impaired in $Bim^{-/-}$ mice [12], we focused on the presence of TCR V β 8⁺ T cells in Peyer's patches by flow cytometric analysis. The number of TCR V β 8⁺ lymphocytes was significantly increased in Peyer's patches from $Bim^{-/-}$ mice compared to wt controls (10.5 ± 1.9 % vs. 7.3 ± 1.2 % respectively, $p < 0.05$; figure 4 A). Increase of TCR V β 8⁺ lymphocytes was confirmed by IF for $Bim^{-/-}$ mice compared to wt control (figure 4 B).

The cytokine profile of mucosal lymphocytes is altered in $Bim^{-/-}$ mice compared to wt animals. Whole Peyer's patches were excised and snap-frozen. We assessed the cytokine profile in whole Peyer's patches without further pre-stimulation of lymphocytes on the level of mRNA. *iNos* gene expression was detectable in wt but almost absent in $Bim^{-/-}$ animals without chronic colitis (1.10 ± 1.00 , $n = 9$ vs. 0.34 ± 0.24 , $n = 12$ respectively, figure 5 A). Difference was significant for wt mice

upon chronic DSS-induced colitis compared to *Bim*^{-/-} animals (1.00 ± 0.97 , $n = 15$ vs. 0.23 ± 0.14 , $n = 17$ respectively, $p < 0.05$; figure 5 A). Data could be confirmed by Western. Wt mice exhibited significantly higher iNOS protein contents than *Bim*^{-/-} mice for both animals without and with chronic DSS-induced intestinal inflammation (0.18 ± 0.04 , $n = 3$, vs. 0.02 ± 0.03 , $n = 5$ respectively for mice without DSS-induced chronic colitis and 0.12 ± 0.08 , $n = 7$, vs. 0.02 ± 0.05 , $n = 6$, $p < 0.05$ respectively for mice with DSS-induced chronic colitis; figure 5 B). For *IL-6*, *TNF*, and *IL-1 β* mRNA expression, no significant changes were recorded between wt and *Bim*^{-/-} mice without and with chronic DSS-induced colitis (not shown).

Discussion

BIM interacts with the pro-survival family member BCL-2. BIM is critically involved in negative selection of thymocytes during maturation processes and BIM plus PUMA co-regulate lymphocyte homeostasis in the periphery [9]. Deletion of activated cells after antigenic challenge is impaired in Bim-deficient animals thereby facilitating the development of systemic lupus erythematosus-like pathology [8]. As dysregulated apoptosis of lymphocytes contributes to the pathogenesis of IBD [14-17, 23] we analyzed the role of BIM in lymphocytes in our mouse model of colitis.

In the present study, we show an impaired removal of autoreactive lymphocytes in *Bim*^{-/-} mice upon chronic DSS-induced colitis. Presence of a significantly increased number of TCR V β 8⁺ lymphocytes in Peyer's patches upon chronic DSS-induced colitis is associated with aggravated mucosal inflammation as determined by significantly increased weight loss and MEICS score of *Bim*^{-/-} compared to wt mice. Data from spleen weight, colon length and histological score confirmed this suggestion. Interestingly, TCR V β 8⁺ lymphocytes can bind SEB. Wt treated with a single intra-rectal instillation of SEB displayed a time- and dose-dependent colonic inflammation which was further significantly increased in ovalbumin transgenic mice with 95 % TCR V β 8⁺ lymphocytes [24].

Enhanced expression of the pro-survival proteins BCL-2 and BCL-x_L was determined in lamina propria T cells of patients with CD when compared with controls. Lamina propria T cells in CD patients show an activation of the STAT-3 signalling pathway mediated by IL-6. Activation of STAT-3 is followed by the induction anti-apoptotic genes such as *BCL-2* and *BCL-x_L* [14]. Resistance of CD T cells to multiple apoptotic signals is associated with increased BCL-2 expression. An abnormal BCL-2 expression in lamina propria mononuclear cells from patients with

CD was demonstrated [15]. A significantly higher BCL-2/BAX ratio in CD mucosa compared to control was reported [16]. These data are consistent with a recent report showing significant resistance to Fas-induced apoptosis of peripheral T-cells from CD patients [17]. The same immunological consequence resulting from the extended lifespan of antigen-primed T cells is supported by a reduced survival or function of Treg cells. Apoptosis is strongly elevated in mucosal and peripheral CD4⁺CD25^{high}Foxp3⁺ Treg cells of patients with IBD [25]. Failure of the apoptotic mechanism of lymphocyte control can lead to the development of autoimmunity or lymphoma.

Bim deficiency perturbed thymic T cell development. As expected for the loss of a pro-apoptotic molecule, the numbers of both the CD4⁻8⁻ pro-T cells and the mature T cells (CD4⁺8⁻ and CD4⁻8⁺) were two- to threefold higher than in wt. Surprisingly, however, the CD4⁺8⁺ pre-T cells, the predominant thymic subpopulation, were only half the normal level. [8].

Interestingly we observed rectum prolapses in *Bim*^{-/-} animals. The trigger for the appearance of prolapses was not investigated in this work. As described for mice homozygous for *Il10*^{tm1Cgn}, targeted mutations leading to altered lymphocyte populations are most likely to be involved in prolapse formation. As described for IL-10^{-/-} mice, animal housing conditions and the microbiome influence prolapse development. However, our mice were housed in IVC in a SPF facility where a less developed microbiome could be expected.

We determined significantly increased inflammation in *Bim*^{-/-} animals compared to wt upon chronic DSS-induced colitis. Absence of BIM is the reason for an impaired removal of autoreactive TCR Vβ8⁺ lymphocytes in Peyer's patches upon chronic DSS-induced colitis. On the other hand, an increase of BIM could have interesting consequences. Activation of Bim-mediated lymphocyte killing upon pro-apoptotic

BH3-mimetics could adjust the balance between activated and regulatory lymphocyte populations and ameliorate colitis. Inducing apoptosis of autoreactive lymphocytes may be a new promising therapeutic strategy for CD patients.

Disclosure:

KL, MK, MF and MH have no conflict of interest to disclose.

GR discloses grant support from Abbot, Ardeypharm, Essex, FALK, Flamentera, Novartis, Roche, Tillots, UCB and Zeller.

References

1. Puthalakath H, Huang DC, O'Reilly LA, King SM, Strasser A. The proapoptotic activity of the Bcl-2 family member Bim is regulated by interaction with the dynein motor complex. *Mol Cell* 1999; **3**:287-96.
2. Ley R, Ewings KE, Hadfield K, Cook SJ. Regulatory phosphorylation of Bim: sorting out the ERK from the JNK. *Cell Death Differ* 2005; **12**:1008-14.
3. Ewings KE, Wiggins CM, Cook SJ. Bim and the pro-survival Bcl-2 proteins: opposites attract, ERK repels. *Cell Cycle* 2007; **6**:2236-40.
4. Kutuk O, Letai A. Displacement of Bim by Bmf and Puma rather than increase in Bim level mediates paclitaxel-induced apoptosis in breast cancer cells. *Cell Death Differ* 2010.
5. Ramjaun AR, Tomlinson S, Eddaoudi A, Downward J. Upregulation of two BH3-only proteins, Bmf and Bim, during TGF beta-induced apoptosis. *Oncogene* 2007; **26**:970-81.

6. Suzuki HI, Kiyono K, Miyazono K. Regulation of autophagy by transforming growth factor-beta (TGF-beta) signaling. *Autophagy* 2010; **6**.
7. Wojciechowski S, Tripathi P, Bourdeau T, Acero L, Grimes HL, Katz JD, Finkelman FD, Hildeman DA. Bim/Bcl-2 balance is critical for maintaining naive and memory T cell homeostasis. *J Exp Med* 2007; **204**:1665-75.
8. Bouillet P, Metcalf D, Huang DC, Tarlinton DM, Kay TW, Kontgen F, Adams JM, Strasser A. Proapoptotic Bcl-2 relative Bim required for certain apoptotic responses, leukocyte homeostasis, and to preclude autoimmunity. *Science* 1999; **286**:1735-8.
9. Tischner D, Woess C, Ottina E, Villunger A. Bcl-2-regulated cell death signalling in the prevention of autoimmunity. *Cell Death Dis* 2010; **1**:e48.
10. Mitchell T, Kappler J, Marrack P. Bystander virus infection prolongs activated T cell survival. *J Immunol* 1999; **162**:4527-35.
11. Hildeman DA, Zhu Y, Mitchell TC, Bouillet P, Strasser A, Kappler J, Marrack P. Activated T cell death in vivo mediated by proapoptotic bcl-2 family member bim. *Immunity* 2002; **16**:759-67.
12. Bouillet P, Purton JF, Godfrey DI, Zhang LC, Coultas L, Puthalakath H, Pellegrini M, Cory S, Adams JM, Strasser A. BH3-only Bcl-2 family member Bim is required for apoptosis of autoreactive thymocytes. *Nature* 2002; **415**:922-6.
13. Tischner D, Gagli I, Peschel I, Kaufmann M, Tuzlak S, Drach M, Thuille N, Villunger A, Jan Wieggers G. Defective cell death signalling along the Bcl-2 regulated apoptosis pathway compromises Treg cell development and limits their functionality in mice. *J Autoimmun* 2012; **38**:59-69.
14. Atreya R, Mudter J, Finotto S, Mullberg J, Jostock T, Wirtz S, Schutz M, Bartsch B, Holtmann M, Becker C, Strand D, Czaja J, Schlaak JF, Lehr HA,

- Autschbach F, Schurmann G, Nishimoto N, Yoshizaki K, Ito H, Kishimoto T, Galle PR, Rose-John S, Neurath MF. Blockade of interleukin 6 trans signaling suppresses T-cell resistance against apoptosis in chronic intestinal inflammation: evidence in crohn disease and experimental colitis in vivo. *Nat Med* 2000; **6**:583-8.
15. Boirivant M, Marini M, Di Felice G, Pronio AM, Montesani C, Tersigni R, Strober W. Lamina propria T cells in Crohn's disease and other gastrointestinal inflammation show defective CD2 pathway-induced apoptosis. *Gastroenterology* 1999; **116**:557-65.
 16. Ina K, Itoh J, Fukushima K, Kusugami K, Yamaguchi T, Kyokane K, Imada A, Binion DG, Musso A, West GA, Dobrea GM, McCormick TS, Lapetina EG, Levine AD, Ottaway CA, Fiocchi C. Resistance of Crohn's disease T cells to multiple apoptotic signals is associated with a Bcl-2/Bax mucosal imbalance. *J Immunol* 1999; **163**:1081-90.
 17. Moret I, Rausell F, Iborra M, Bastida G, Aguas M, Tortosa L, Nos P. aus DDW Gastro Supplement. *Gastroenterology* 2012; **142**:S-877.
 18. Labi V, Erlacher M, Kiessling S, Manzl C, Frenzel A, O'Reilly L, Strasser A, Villunger A. Loss of the BH3-only protein Bmf impairs B cell homeostasis and accelerates gamma irradiation-induced thymic lymphoma development. *J Exp Med* 2008; **205**:641-55.
 19. Obermeier F, Kojouharoff G, Hans W, Scholmerich J, Gross V, Falk W. Interferon-gamma (IFN-gamma)- and tumour necrosis factor (TNF)-induced nitric oxide as toxic effector molecule in chronic dextran sulphate sodium (DSS)-induced colitis in mice. *Clin Exp Immunol* 1999; **116**:238-45.

20. Becker C, Fantini MC, Wirtz S, Nikolaev A, Kiesslich R, Lehr HA, Galle PR, Neurath MF. In vivo imaging of colitis and colon cancer development in mice using high resolution chromoendoscopy. *Gut* 2005; **54**:950-4.
21. Steidler L, Hans W, Schotte L, Neiryneck S, Obermeier F, Falk W, Fiers W, Remaut E. Treatment of murine colitis by *Lactococcus lactis* secreting interleukin-10. *Science* 2000; **289**:1352-5.
22. Hubner A, Cavanagh-Kyros J, Rincon M, Flavell RA, Davis RJ. Functional cooperation of the proapoptotic Bcl2 family proteins Bmf and Bim in vivo. *Mol Cell Biol* 2010; **30**:98-105.
23. Kruidenier L, Kuiper I, Van Duijn W, Mieremet-Ooms MA, van Hogezaand RA, Lamers CB, Verspaget HW. Imbalanced secondary mucosal antioxidant response in inflammatory bowel disease. *J Pathol* 2003; **201**:17-27.
24. Lu J, Wang A, Ansari S, Hershberg RM, McKay DM. Colonic bacterial superantigens evoke an inflammatory response and exaggerate disease in mice recovering from colitis. *Gastroenterology* 2003; **125**:1785-95.
25. Veltkamp C, Anstaett M, Wahl K, Moller S, Gangl S, Bachmann O, Hardtke-Wolenski M, Langer F, Stremmel W, Manns MP, Schulze-Osthoff K, Bantel H. Apoptosis of regulatory T lymphocytes is increased in chronic inflammatory bowel disease and reversed by anti-TNFalpha treatment. *Gut* 2011; **60**:1345-53.

Figure legends

Figure 1: *Bim*^{-/-} mice spontaneously developed anal bleeding and rectum prolapses.

(A) Prolapse in *Bim*^{-/-} mice. Genotyping of *Bim*^{-/-} mice. (B) Quantification of prolapses.

Figure 2: *Bim*^{-/-} mice develop an aggravated chronic DSS-induced colitis compared to wt. (A) Percental body weight loss (\pm SD). (B) Statistical analysis of colonoscopy score (MEICS). Colonoscopy was performed on the day prior to sacrificing the animals. Representative images demonstrate colonoscopy pictures derived from DSS-treated wt mice and *Bim*^{-/-} mice. * $p < 0.05$.

Figure 3: *Bim*^{-/-} mice develop an aggravated chronic DSS-induced colitis. (A) Statistical analysis of spleen weight per body weight. (B) Statistical analysis of colon length and representative images. (C) Histoscore derived from water- (n = 4) or DSS-treated (n = 5) wt and water- (n = 7) or DSS-treated (n = 7) *Bim*^{-/-} mice. (D) *Bim* is increased in Peyer's patches in wt mice upon chronic DSS. * $p < 0.05$, ** $p < 0.01$.

Figure 4: Impaired removal of autoreactive lymphocytes in *Bim*^{-/-} upon chronic DSS-induced colitis. (A) Flow-cytometric analysis of TCR V β 8⁺ lymphocytes isolated from murine Peyer's patches and statistical analysis, TCR V β 8⁺ lymphocytes are shown as percentage from the total number of isolated cells (* $p < 0.05$, Bonferroni t-test, n = 6 each). (B) IF for TCR V β 8⁺ in sections from Peyer's patches from wt and *Bim*^{-/-}.

Figure 5: iNOS expression in whole Peyer's patches. (A) iNOS RNA expression. (B) iNOS protein expression.

Figure 1

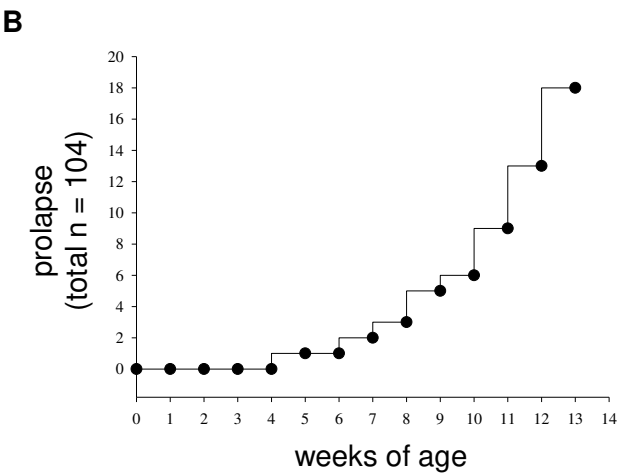
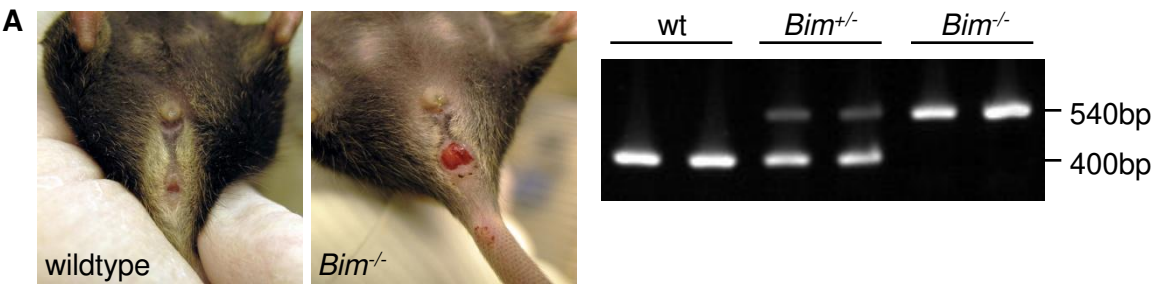


Figure 2

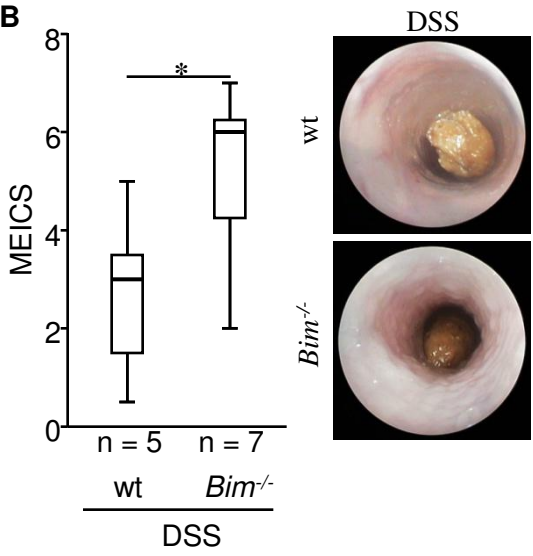
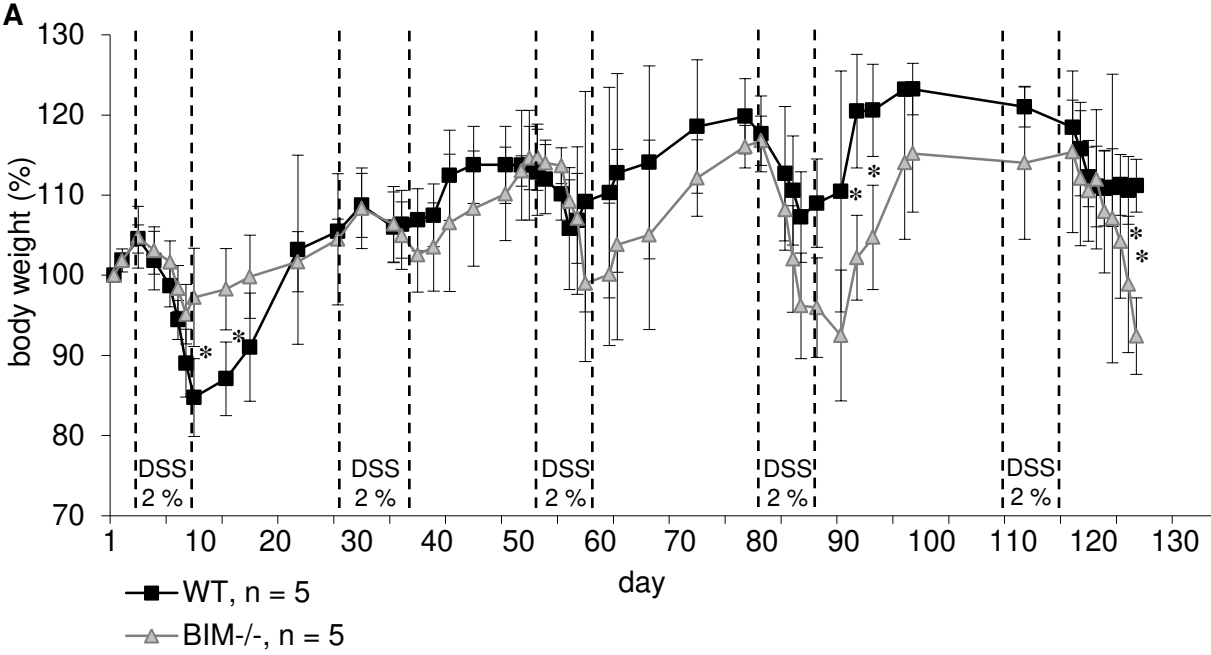


Figure 3

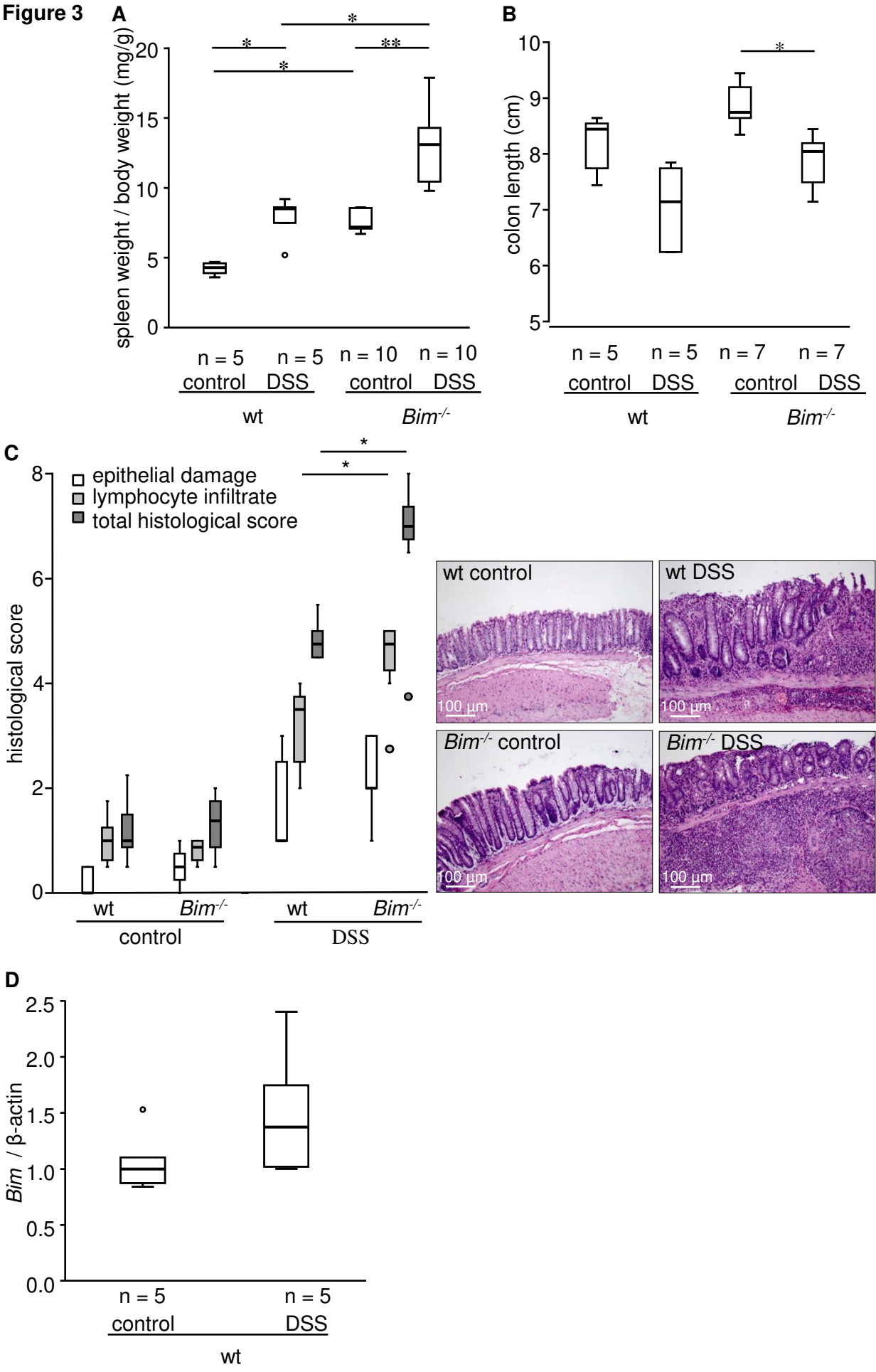


Figure 4

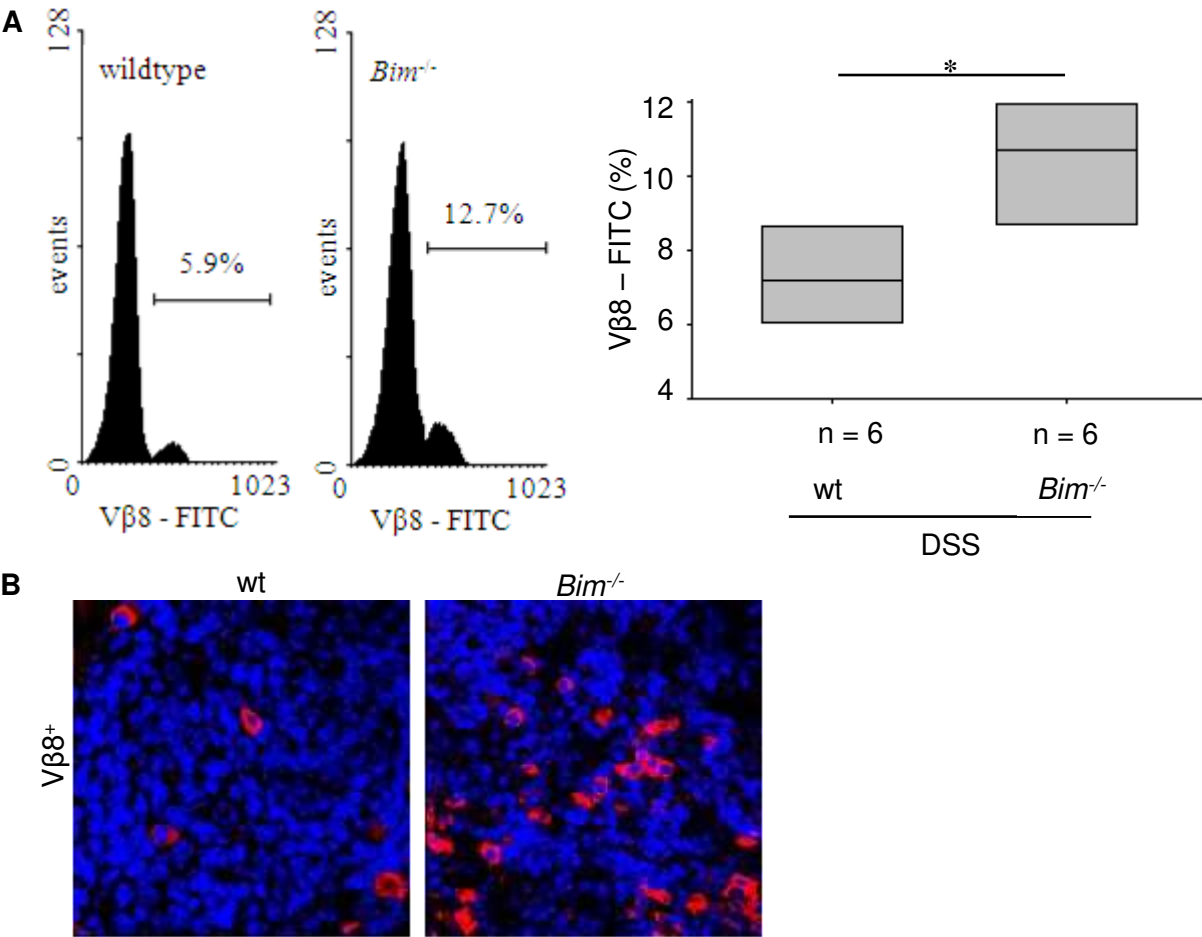
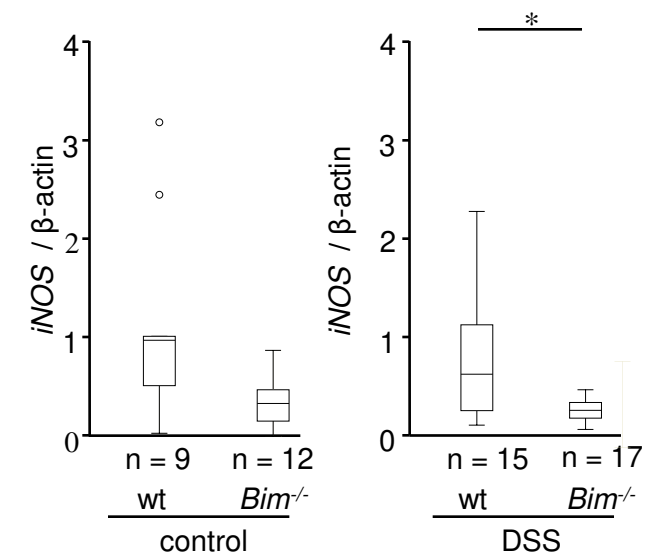


Figure 5

A



B

